



Article

Heteropolyacid Incorporated Bifunctional Core-Shell Catalysts for Dimethyl Ether Synthesis from Carbon Dioxide/Syngas

Birce Pekmezci Karaman ¹, Nuray Oktar ^{1,*}, Gülşen Doğu ¹ and Timur Dogu ^{2,*}¹ Chemical Engineering Department, Gazi University, Ankara 06570, Turkey² Chemical Engineering Department, Middle East Technical University, Ankara 06800, Turkey

* Correspondence: nurayoktar@gazi.edu.tr (N.O.); tdogu@metu.edu.tr (T.D.)

Abstract: Core-shell-type catalysts, which are synthesized by encapsulating the Cu-ZnO-Alumina type methanol synthesis catalyst (CZA) by silicotungstic acid (STA)-incorporated mesoporous alumina, were prepared following a hydrothermal route and tested in DME synthesis from syngas and CO₂. Activity tests, which were performed in the pressure range of 30–50 bar, and the temperature range of 200–300 °C, with different feed compositions (CO₂/CO/H₂: 50/-/50, 40/10/50, 25/25/50, 10/40/50) showed that the best-operating conditions for the highest DME yield were 275 °C and 50 bar. Results proved that the presence of CO₂ in the syngas had a positive effect on the DME yield. The total conversion of CO + CO₂ increased with an increase in CO₂/CO ratio. An overall conversion of CO + CO₂ and DME selectivity values were obtained as 65.6% and 73.2%, respectively, with a feed composition of H₂/CO₂/CO = 50/40/10. Synthesis of methanol using the CZA catalyst from the CO₂-containing gas mixtures was also investigated, and the total conversion of CO + CO₂ and methanol selectivity values of 32.0% and 83.6%, respectively, were obtained with the H₂/CO₂/CO = 50/40/10 gas mixture. Results proved that the new STA incorporated core-shell-type bifunctional catalysts were highly promising for the conversion of CO₂-containing syngas to DME.

Keywords: dimethyl ether; methanol; carbon dioxide; core-shell catalyst; silicotungstic acid



Citation: Karaman, B.P.; Oktar, N.; Doğu, G.; Dogu, T. Heteropolyacid Incorporated Bifunctional Core-Shell Catalysts for Dimethyl Ether Synthesis from Carbon Dioxide/Syngas. *Catalysts* **2022**, *12*, 1102. <https://doi.org/10.3390/catal12101102>

Academic Editors: Hugo de Lasa and Mohammad Mozahar Hossain

Received: 31 August 2022

Accepted: 20 September 2022

Published: 23 September 2022

Publisher's Note: MDPI stays neutral with regard to jurisdictional claims in published maps and institutional affiliations.



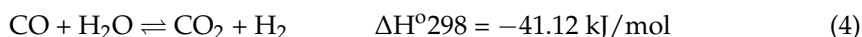
Copyright: © 2022 by the authors. Licensee MDPI, Basel, Switzerland. This article is an open access article distributed under the terms and conditions of the Creative Commons Attribution (CC BY) license (<https://creativecommons.org/licenses/by/4.0/>).

1. Introduction

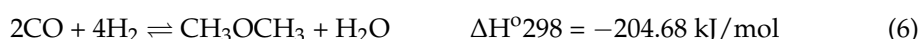
Diminishing fossil fuel usage and greenhouse gas emissions depend on the production of environmentally friendly new energy carriers [1–4]. Dimethyl ether (DME) has gained significant interest as an alternative fuel. It has a high cetane number of 55–60 compared with diesel fuel (45–50). Moreover, DME burns with the emission of no particulate matter, no SO_x, and less NO_x than conventional diesel fuel. Therefore, DME is considered as an attractive and promising clean fuel alternative for diesel engines [5–7].

Dimethyl ether can be produced from carbon dioxide-rich syngas. Raw materials of syngas are natural gas, coal, crude oil, waste materials, and biomass. CO₂-rich syngas is produced as an intermediate for DME production via reforming and gasification reactions. The syngas, which can be produced by a gasification/reforming reaction, can then be converted to DME following two synthesis routes. One is the indirect synthesis method, and the other one is the direct synthesis method. The indirect process is carried out in two separate reactors, which consist of a methanol synthesis reactor from syngas and the subsequent methanol dehydration reactor to produce DME. Cu-ZnO-based catalysts are generally used as methanol synthesis catalysts, and solid acid catalysts are preferred for the methanol dehydration reaction.





In the direct synthesis of DME, reactions (1–4) take place in a single reactor, and DME is synthesized directly from syngas [8–12]. In this reaction system, Cu-ZnO-based catalysts and acidic catalysts are used simultaneously. Methanol synthesis reaction (Equation (1)) has equilibrium limitations. However, the direct synthesis of DME reaction overcomes these limitations and increases CO conversion. Cu-ZnO-based materials also facilitate the water–gas shift reaction. The overall stoichiometry of direct synthesis of DME (Equations (5) and (6)) includes methanol synthesis (Equations (1) and (2)), methanol dehydration (Equation (3)), and water–gas shift reactions (WGS) (Equation (4)) [13–15].



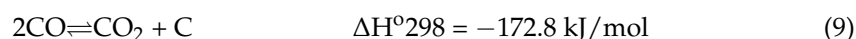
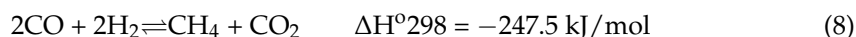
Many recent studies investigated the effect of feed composition on DME selectivity. DME synthesis from CO₂-rich syngas allows the utilization of CO₂, which is one of the most abundant greenhouse gases [12–18]. Thus, the use of DME as a diesel fuel alternate has the potential to help reduce global warming as well as air pollution. The overall stoichiometry of the direct DME synthesis from CO₂ is given in Equation (7). Compared to the CO hydrogenation for DME production (Equations (5) and (6)), the formation of DME from the CO₂ (Equation (7)) requires an extra amount of hydrogen in the feed stream, and water is produced as a by-product. Hence, the reverse water–gas shift (RWGS) reaction becomes significant during the DME production via CO₂ hydrogenation reaction. The thermodynamic analysis results of the CO₂ hydrogenation reaction are not as favorable as that of the CO hydrogenation process [16,17]. Ateka et al. conducted a thermodynamic analysis of methanol and DME synthesis from a gas mixture of CO₂/CO/H₂ at different reaction temperatures (200–400 °C) and pressure values (10–100 bar). The results indicated that the low DME selectivity was related to the low equilibrium constant of the methanol formation from CO₂ + H₂ [16]. Moreover, the formation of DME is controlled by the RWGS reaction. However, the addition of a certain amount of CO₂ to the CO + H₂ feed stream considerably increases the DME selectivity. Bayat et al. investigated the direct synthesis of dimethyl ether over admixed catalysts [14]. The admixed catalyst contains silicotungstic acid-incorporated mesoporous alumina catalyst (STA@MA) and copper-based methanol synthesis catalyst (MRC). This study showed that the STA incorporated catalyst indicated promising dehydration activity for DME production from CO₂-containing syngas. The overall conversion of CO + CO₂ and DME selectivity increased with an increase in the amount of CO₂ in the feed stream. In the study by Çelik et al. [15], DME synthesis was achieved by using physical mixtures of TRC-75 type solid acid catalyst and Cu-Zn-based materials (MRC). The presence of CO₂ in the feed stream increased the DME selectivity. A comprehensive review of recent advances in the direct synthesis of DME from CO₂ is reported by Mota et al. [18]. As a result of these studies, it can be said that the selection of the dehydration catalyst and feed conditions are highly effective on DME selectivity and overall conversion of (CO + CO₂).



In the literature, considerable attention has been paid to the design of the bifunctional catalysts for DME production. Commonly, Cu/ZnO/Al₂O₃ and Cu/ZnO/ZrO₂ catalysts are used in the methanol synthesis reaction [18–23]. The active phase in the methanol synthesis catalysts is metallic copper. Promoters are also used to enhance the activity of Cu-based catalysts. The promoters of the methanol synthesis catalysts are selected according to the feed composition and reaction conditions. As methanol production is conducted with CO₂-rich syngas, zirconia promoters indicate promising activity in terms of CO/CO₂ conversion and MeOH selectivity [20,23].

Al₂O₃ promoters show high catalytic activity in CO hydrogenation reaction for MeOH synthesis. Our previous study indicated that methanol selectivity and CO conversion were highly dependent on Cu/ZnO/Al₂O₃ and Cu/Zn/ZrO₂ molar ratio [22]. As far as methanol selectivity and product distribution were concerned, the best catalytic performance was obtained with the CZA:631 catalyst. The addition of ZnO to the methanol synthesis catalysts promotes the dispersion of Cu. Therefore, a decrease in the amount of ZnO increased the particle diameter of copper and caused a lower catalytic activity. Furthermore, Cu/Zn/Al catalysts indicated superior activity compared to Cu/Zn/Zr catalysts in the CO hydrogenation reaction for MeOH synthesis [22]. To increase the catalytic activity of the CZA catalysts, metal oxides such as TiO₂ [24], Ga₂O₃ [25], CeO₂ [26], etc., have also been incorporated into the catalyst structure. The addition of metal oxides to the structure enhances the thermal activity of the catalyst and prevents the sintering of copper at high temperatures.

In the direct synthesis of the DME process, the surface acidity of methanol dehydration catalysts affects the product distribution highly. The catalysts with a high Bronsted acidity show high DME selectivity and overall CO + CO₂ conversion. However, due to the reaction mechanism of the direct synthesis process, dehydration catalysts are expected to have the Lewis acid sites as well as the Bronsted acid sites. In the DME production, the first step of the methanol production from syngas takes place on the Lewis acid site of the bifunctional catalysts. Methanol, thus produced, is then converted to the DME on the Bronsted acid sites [22,27]. For this reason, the improved intensity of Bronsted acid sites enables an increase in DME selectivity and CO + CO₂ conversion. Furthermore, the high Lewis sites activate the undesired reactions. Reverse dry reforming (Equation (8)) and Boudouard reaction (Equation (9)) may also take place during DME synthesis from syngas. Reverse dry reforming reaction is an exothermic reversible reaction. From the thermodynamics point of view, the reaction temperature and pressure of the DME synthesis process are quite favorable for the occurrence of reverse dry reforming reaction. In fact, the equilibrium conversion of CO to CH₄ through the reverse dry reforming reaction (Equation (8)) is even more favorable than the methanol synthesis reaction at temperatures lower than 400 °C. However, mainly Ni and noble metals were reported as active metals used for this reaction. CZA-type methanol synthesis catalyst is not expected as active as Ni for the reverse dry reforming reaction. As reported in the literature, the incorporation of noble and non-noble metals into the support materials may create a synergistic effect, leading to the reverse of the methane reforming reaction [28]. Hence, the formation of some methane is expected to form as an undesired side product during the direct synthesis of DME from syngas. Furthermore, as a result of the occurrence of the Boudouard reaction, coke formation may occur on the catalyst surface, which causes the catalyst deactivation (Equation (9)).



Heteropolyacids (HPAs) were used as promoters to enhance the Bronsted acidity of the catalyst in recent studies. HPAs have very strong Bronsted acidity and a structure with very high proton mobility. Among the HPAs, silicotungstic acid (STA) has shown higher activity in dimethyl ether and diethyl ether production compared to tungstophosphoric acid TPA. Also, STA has shown higher stability at temperatures over 200 °C [22,27–29]. For this reason, STA was selected as the solid acid source used for the dehydration catalyst in the present study.

The catalysts used for DME production are commonly prepared as a physical mixture of methanol synthesis and dehydration catalysts. However, admixed catalysts have some disadvantages. During the preparation step, these catalysts may not be homogeneously mixed. Thus, some side reactions may occur, and the selectivity of the main product may decrease. As a result, increased attention has been paid to the development of core-shell model catalysts in recent years for the direct synthesis of DME. Some studies have

demonstrated that CuO-ZnO-Al₂O₃@HZSM-5 [30,31], CuO-ZnO-Al₂O₃@SiO₂-Al₂O₃ [32], CuO-ZnO-ZrO₂@SAPO-11 [19] and tungstophosphoric acid-incorporated catalysts [33] showed promising activity for DME production. However, a high amount of coke was formed with zeolite-based Si-Al content catalysts mainly due to their high Lewis acidity. Contador et al. investigated the catalytic activity of CuO-ZnO-ZrO₂@SAPO-11 core-shell catalysts on the direct synthesis of dimethyl ether (DME) from CO + CO₂ hydrogenation [19]. That study showed that methanol synthesis and water-gas shift reactions occur in the core section of the catalyst, and DME production is achieved on the shell side. Hence, the methanol synthesis and DME formation reactions take place at different zones of the core-shell-type catalyst.

High water concentration may cause hydrothermal degradation of methanol synthesis catalysts [34]. This is one of the reasons for the deactivation of CZA catalysts during the synthesis of DME from syngas. As reported in the literature, CZA catalysts may lose a large percentage of their activity within the first 1000 h of operation [34]. In the case of the core-shell-type catalysts, the dehydration reaction takes place in the shell section of the catalyst. Hence, the significance of the interaction of the water produced in the shell section, which the CZA in the core section of the catalyst will diminish. This will prevent the deactivation of CZA by hydrothermal degradation. Moreover, core-shell-type catalysts showed good resistance to the sintering of Cu species at high reaction temperatures. The incorporation of both functions in the core-shell catalyst enhanced the synergy of the reactions. Methanol formed in the core section passes to the acidic shell side and then produces DME. Thus, the selectivity of DME and the overall conversion (CO + CO₂) increase [30–32].

The first objective of this study was to develop a novel core-shell-type catalyst for the direct synthesis of DME. In this core-shell-type catalyst, the CZA catalyst was encapsulated by STA incorporated mesoporous alumina. The effect of STA incorporation on the performance of the catalyst was investigated by synthesizing catalysts having different amounts of silicotungstic acid. The second objective was to examine the effects of feed composition, reaction temperature, and pressure on the performance of this novel core-shell-type catalyst. The third objective was to be able to use CO₂ as a carbon source in the synthesis of DME using this novel catalyst. Hence, in the present study, core-shell-type catalysts, which are synthesized by encapsulating the Cu-ZnO-Alumina type methanol synthesis catalyst by mesoporous alumina (MA), were prepared following a hydrothermal route. The catalytic performance of STA incorporated (CZA-MA) core-shell catalysts was then investigated in the direct synthesis of DME from syngas and CO₂. STA@CZA-MA catalysts are novel in terms of both the synthesis method and their use in the direct synthesis of DME. Initial experiments were performed to investigate the performance of these STA incorporated core-shell-type catalysts in the hydrogenation of CO. Then, activity test studies were performed in the pressure range of 30–50 bar and the temperature range of 200–300 °C, with different feed compositions (CO₂/CO/H₂: 50/-/50, 40/10/50, 25/25/50, 10/40/50). One goal of this study was to determine the optimum reaction conditions for obtaining high DME selectivity. Another goal was to convert the most significant greenhouse gas, which is CO₂, to fuel alternates. Furthermore, in the studies examining the effect of feed composition on product distribution, methanol synthesis studies with a CZA catalyst were also conducted using CO₂ as the carbon source. In this regard, detailed information on the characterization results of the catalysts and thermodynamic analysis of DME production were also obtained.

2. Results and Discussion

2.1. Textural and Structural Properties of Core-Shell Model STA- Incorporated CZA-MA Catalysts

Core-shell-type catalysts, which were synthesized in this work, were calcined at 750 °C to obtain the γ -alumina form of the shell section, which is the most acidic phase of the alumina. However, it has been stated in the literature that CuO structures may sinter above 300 °C [15,33]. To check the effect of calcination temperature on the structure of the core section of the bi-functional catalyst, namely the methanol synthesis catalyst, it was calcined at both 350 °C and 750 °C (CZA-350 and CZA-750), and the change in its

physical properties was examined. The XRD patterns of CZA-350 and CZA-750 are given in Figure 1a. The XRD patterns of the core-shell-type CZA-MA catalyst are also given in the same figure. In the XRD analysis of the CZA catalyst (CZA-350) calcined at 350 °C, characteristic peaks of CuO and ZnO were observed. The main peaks of CuO (JCPDS File No: 05-0661) were determined at 2θ values of 35.2, 38.5, 48 and 62.5, and the main peak of ZnO (JCPDS File No: 36-1451) was observed at 2θ : 31.7 [22]. The peaks of Al_2O_3 (JCPDS File No.: 29-0063) could not be observed in the structure of this CZA catalyst [35–37]. This result was explained by the homogeneous distribution of Al_2O_3 in the catalyst structure. However, the diffraction peaks of CuO and ZnO became more intense with the increment of the calcination temperature. This result could be explained by the sintering of metals at the high calcination temperature. Also, unlike the CZA-350 catalyst, Cu and Zn metals interacted with alumina in the CZA-750 catalyst to form CuAl_2O_4 and ZnAl_2O_4 alloys [38]. The crystal size of the CuO particles was calculated using the main characteristic peak of the CuO at 2θ : 35.6°. Using Scherrer's equation, the CuO crystal sizes in the structures of the CZA-350 and CZA-750 catalysts were found as 5.89 nm and 21.89 nm, respectively.

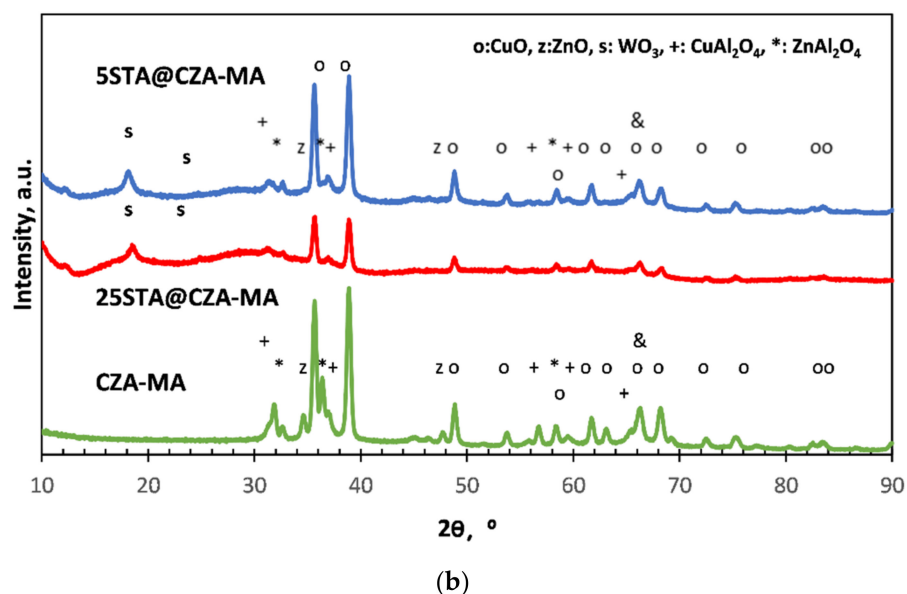
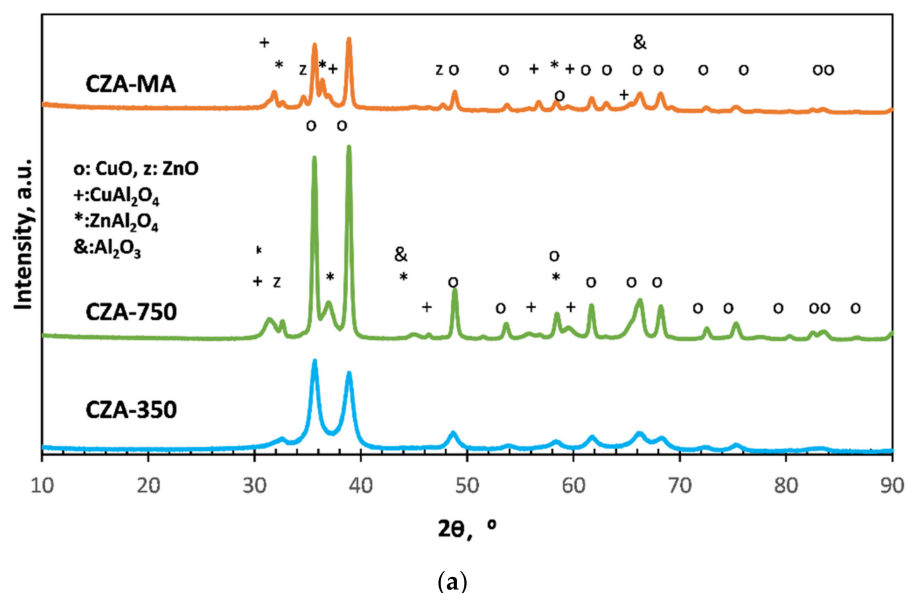


Figure 1. (a) XRD patterns of methanol synthesis catalysts and core-shell model catalyst, (b) XRD patterns of STA incorporated core-shell model catalysts.

The XRD result of the core-shell-type CZA-MA catalyst is quite similar to the CZA-750 catalyst, but the intensity of the peaks of CuO and ZnO are lower. The CuO crystal size in the structure of the calcined core-shell-type CZA-MA catalyst was found as 11.4 nm, which was about half of the CuO crystal size of the CZA-750 catalyst. This result indicated that the alumina layer that coated the methanol synthesis catalyst prevented the sintering of the CuO and ZnO at high temperatures.

The XRD analysis results of the STA incorporated CZA-MA catalyst are given in Figure 1b. Our previous study had shown that the Kegging structure of STA somewhat deteriorated after the impregnation step, while some WO_x structures were formed [22]. The absence of the peak at a 2 θ value of 26° indicated that there was no STA structure present in the core-shell-type catalyst [27,28]. However, the small diffraction peaks at 18°, 23.2°, and 26.7° were referred to WO₃ clusters. In addition, the characteristic peaks of CZA-MA catalysts were also appearing. This result showed that the main structures of CZA-MA catalysts were preserved after the impregnation step of silicotungstic acid.

The reduction properties of the CZA-350 and core-shell-type CZA-MA catalysts were investigated by the H₂-TPR analysis technique. As seen in Figure 2, TPR profiles of calcined CZA and CZA-MA catalysts have two reduction peaks, corresponding to CuO and ZnO, respectively. In the case of the CZA-350 catalyst, the maximum of the CuO reduction peak appeared at 300 °C, while the maximum of the broad reduction peak of the ZnO was observed at about 600 °C. In the case of the core-shell-type CZA-MA catalyst, the reduction temperature of CuO increased, and the maximum of that peak shifted to 350 °C. This result showed that the core-shell structure protected the CuO in the core against sintering, thus increasing its thermal stability.

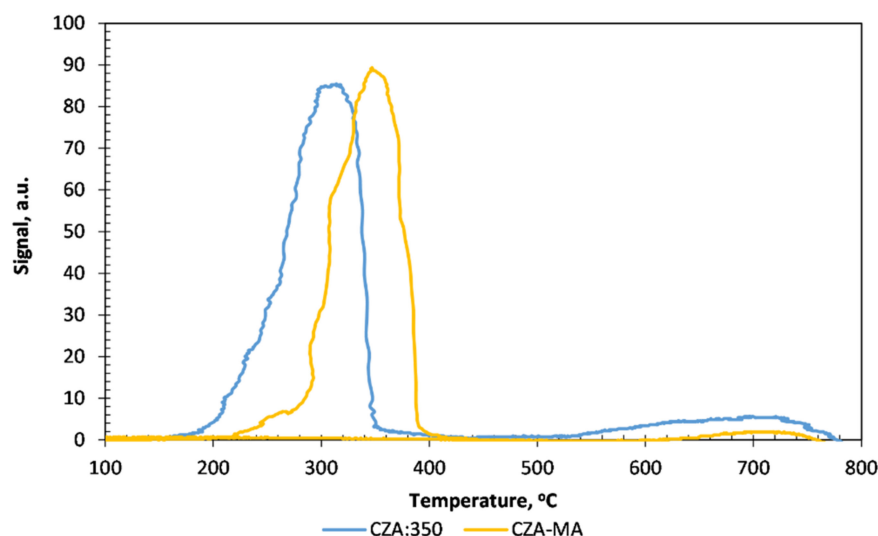
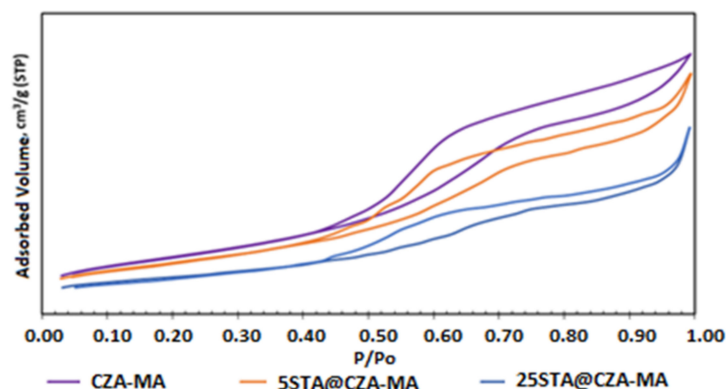


Figure 2. TPR analysis results of CZA:350 and CZA-MA.

The physical properties of STA incorporated core-shell-type catalysts are listed in Table 1. The surface area of the CZA-MA catalyst was around 163 m²/g with a mean pore diameter of 7.4 nm. For STA incorporated, some decrease in surface area was observed with an increase in the amount of STA. The surface area of 25STA@CZA-MA was determined as 130 m²/g. The mean pore diameter of CZA-MA was also decreased from 7.4 nm to 6.2 nm as a result of STA impregnation (25%). These results showed that most of the STA were penetrated into the pores and deposited on the surfaces of the CZA-MA catalysts. The N₂ physisorption (Figure 3) of the STA@CZA-MA catalysts are similar to a Type-IV isotherm, indicating the presence of mesoporous structures with ordered pores. After the incorporation of STA, hysteresis loops were obtained with lower intensity, indicating some disturbance of the pores. Moreover, the hysteresis loops shifted to lower partial pressures because of the decrease in the pore diameters of the catalysts.

Table 1. Some physical properties of STA incorporated core-shell model catalysts.

Catalyst	Surface Area (m ² /g)	Pore Diameter, nm	Pore Volume, cm ³ /g	SEM-EDS	ICP-MS
CZA-MA	163	7.4	0.60	—	—
5STA@CZA-MA	155	6.8	0.55	3.5	4.1
25STA@CZA-MA	130	6.2	0.43	22	21.4

**Figure 3.** N₂ physisorption of STA incorporated core-shell model catalysts.

SEM images of CZA-MA catalysts are given in Figure 4. From the SEM images of the catalysts, it could be seen that the surface morphologies of the catalysts did not significantly change as a result of STA impregnation. The distribution of the silicotungstic acid on the CZA-MA catalysts was observed from the BSD-SEM images (backscattered scanning electron images). As known from the literature, the active metal with a large atomic mass appears brighter in BSD photographs. Lee et. al., investigated lithium dispersion on the LLZTO electrolyte with BSD-SEM images. The study revealed that the brighter and darker areas correspond to high atomic number elements (e.g., Zr and La) and low atomic number elements (e.g., Li), respectively [39]. Moreover, the distribution of STA on the catalyst surface was also investigated in our previous studies using the BSD-SEM images [22,28]. Tungsten in the STA has the highest atomic mass, so it could be easily observed as brighter spots in Figure 4c,e. These images indicated that STA was uniformly dispersed into the catalyst.

Chemical analysis of the catalysts was conducted by the Energy-Dispersive X-ray spectroscopy (EDS) and Inductively Coupled Plasma Mass Spectrometer (ICP-MS) analysis techniques. The EDS and ICP-MS (Table 1) analysis results indicated that the amount of heteropoly acid on the catalyst surface was close to the values in the synthesis solution (5 and 25% by mass). These results showed that the heteropoly acid was successfully loaded into the catalyst structure.

Diffuse reflectance FTIR analyses of pyridine-adsorbed catalysts (Figure 5) were performed to determine the type of surface acidity. DME selectivity and overall conversion are expected to increase with an increase in the Bronsted acidity of the catalyst. However, the presence of Lewis acid sites led to coke formation and facilitated the side reactions. The characteristic peaks of Lewis acid sites are at wavelengths 1445–1450 and 1600–1630 cm⁻¹, and the peaks at wavelengths of 1540 and 1640 cm⁻¹ are assigned to Bronsted acid sites. The peak at the 1490 cm⁻¹ wavelength belongs to both Lewis and Bronsted acid sites [28]. As reported in our previous studies, mesoporous alumina catalyst has the Lewis acid sites at 1445 and 1590 cm⁻¹ [5]. Similar to the mesoporous alumina catalyst, the CZA-MA catalyst also has Lewis acid sites, and there is no band corresponding to the Bronsted acid sites. However, the Bronsted acid sites were observed with the addition of STA into the CZA-MA. The intensity of the peaks at 1640 cm⁻¹ increased with the increase in the amount of STA. Moreover, 25STA@CZA-MA catalyst showed higher Bronsted acidity than 5STA@CZA-MA catalyst.

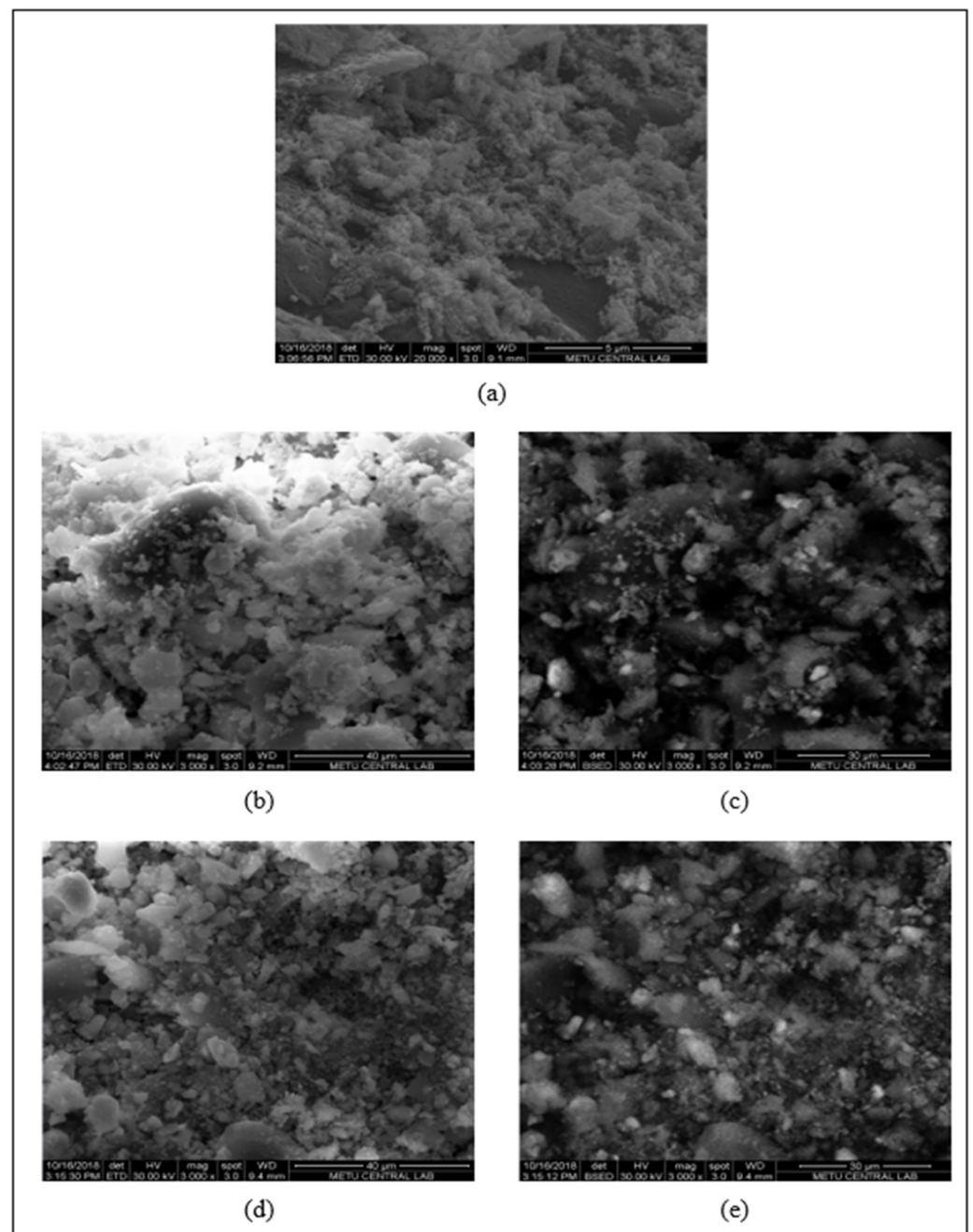


Figure 4. SEM images of (a) CZA-MA, (b) 5STA@CZA-MA, and (d) 25STA@CZA-MA. BSD-SEM images of (c) 5STA@CZA-MA ve, and (e) 25STA@CZA-MA.

High-resolution TEM images for the core-shell-type CZA-MA catalyst are displayed in Figure 6. As can be observed in these figures, the core-shell structure was established. The methanol synthesis catalyst of CZA cores was entirely encapsulated by the mesoporous alumina shells.

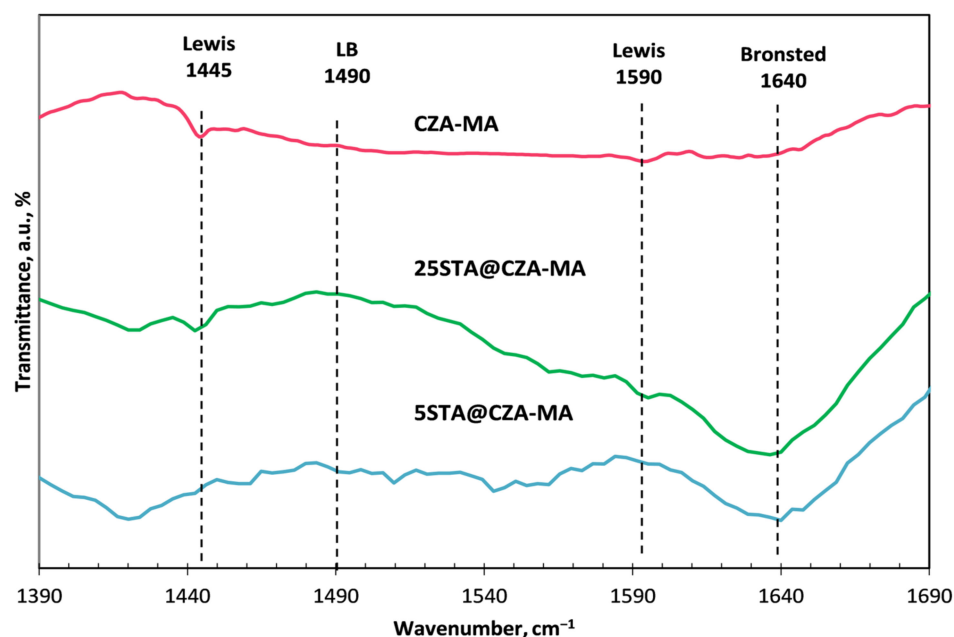


Figure 5. DRIFT spectra of the STA incorporated core-shell catalysts.

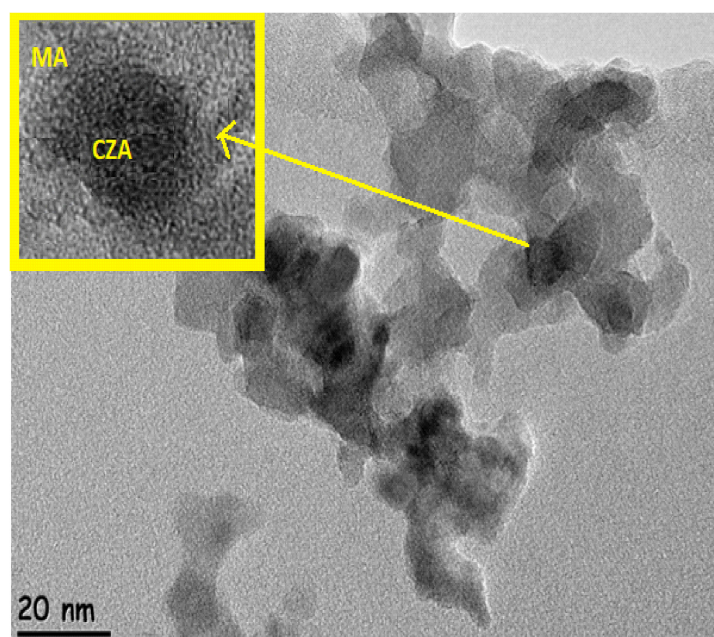


Figure 6. HR-TEM images of the CZA-MA catalyst.

2.2. Direct Synthesis of DME from Syngas in the Absence of CO_2

As known from the literature, the feed molar ratio of the syngas is an important factor for DME selectivity [40]. According to the stoichiometry of the overall DME synthesis reaction (Equation (5)), the CO/H_2 ratio should be 1/1 in the feed stream. Hence, this ratio was selected in our study in the investigation of DME synthesis from $\text{CO} + \text{H}_2$ mixtures. In the literature, Erena et al. investigated the effect of the H_2/CO molar ratio of the feed stream using different values of this ratio as 1/1, 2/1, 4/1, 6/1, and 8/1. In that study, reaction temperature and pressure were adjusted as 275 °C and 40 bar, respectively. The results showed that the increase in H_2/CO molar ratio had a positive effect on DME selectivity and CO conversion. For the $\text{H}_2/\text{CO} = 2/1$ ratio, the maximum CO selectivity was obtained [40].

The activity of STA incorporated CZA-MA catalysts was tested in the direct synthesis of DME reaction. Fractional conversion of CO and the selectivities of the prod-

ucts (DME, methanol, carbon dioxide) were evaluated from the experimental data using Equations (10)–(13). Note that in the experiments performed with a feed stream containing only CO and H₂ as the reacting species, CO₂ is a product. However, in the case of using a feed stream containing both CO and CO₂, carbon dioxide may also be the source of carbon to produce methanol and DME.

$$\text{CO conversion} = \frac{F_{\text{CO}_{in}} - F_{\text{CO}_{out}}}{F_{\text{CO}_{in}}} \quad (10)$$

$$\text{DME selectivity} = \frac{2 \times F_{\text{DME}}}{F_{\text{CO}_{in}} - F_{\text{CO}_{out}}} \quad (11)$$

$$\text{Methanol selectivity} = \frac{F_{\text{MeOH}}}{F_{\text{CO}_{in}} - F_{\text{CO}_{out}}} \quad (12)$$

$$\text{Carbon dioxide selectivity} = \frac{F_{\text{CO}_2}}{F_{\text{CO}_{in}} - F_{\text{CO}_{out}}} \quad (13)$$

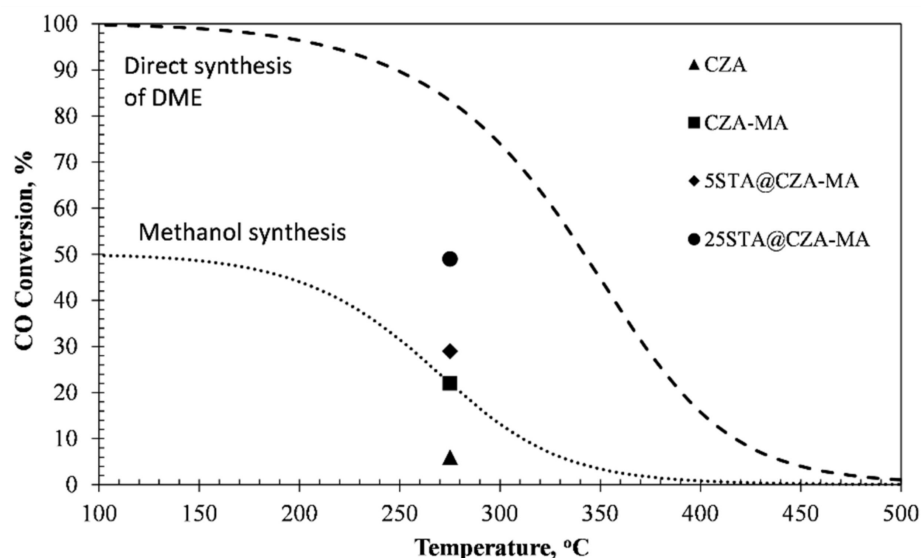
Activity test results obtained with a feed stream composition of CO/H₂ = 1/1 (no CO₂ in the feed stream) using the STA incorporated core-shell catalysts are given in Table 2. CO conversion of CZA-MA catalyst was obtained as 22%. Direct synthesis of the DME reaction eliminated the thermodynamic limitation of the methanol synthesis reaction, which resulted in an increase in CO conversion. For the CZA catalyst, the average CO conversion was approximately 5% [22]. When the CZA catalyst was encapsulated with mesoporous alumina, the average CO conversion value increased by approximately 4 times to 22%. Moreover, as for the STA incorporated catalysts, CO conversion increased up to 49%. CO conversion values obtained with CZA, CZA-MA, the STA-impregnated core-shell-type catalysts and the equilibrium conversion values are presented in Figure 7a. Equilibrium calculations were performed using an algorithm that was based on minimizing the Gibbs free energy. Due to the synergistic effect of the methanol dehydration reaction, the conversion values of CO in the DME synthesis reaction are much higher than the equilibrium conversion of the methanol synthesis reaction (Figure 7a). Also, both of the STA incorporated catalysts showed stable catalytic performance within a reaction period of 200 min (Figure 7b). In order to check the catalyst stability in longer reaction periods, time-on stream tests extending to longer reaction times may be performed.

Table 2. Activity Test Results of the STA incorporated core-shell catalysts (T = 275 °C; P = 50 bar; CO/H₂:1/1 as feed stream) (Duration of reaction period: 200 min).

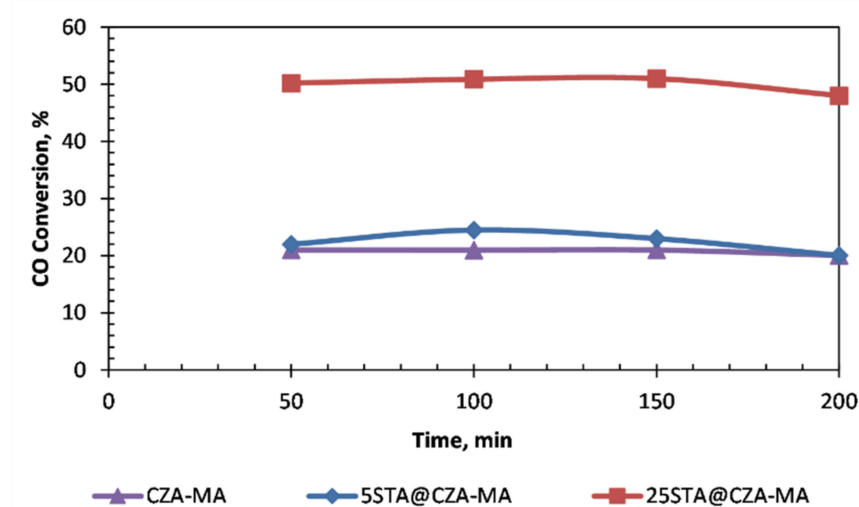
Catalyst	CO Conversion, %	CH ₄ Selectivity, %	CO ₂ Selectivity, %	MeOH Selectivity, %	DME Selectivity, %
CZA-MA	22	0.2	30.3	17.0	52.5
5STA@CZA-MA	29	0.5	36.0	12.0	51.5
25STA@CZA-MA	49	0.4	31.8	8.0	59.8

As presented in Table 2, the highest DME selectivity was achieved with the 25STA@CZA-MA catalyst, as 59.8%. The corresponding methanol selectivity was only 8%, indicating that most of the methanol produced in the core section was dehydrated, yielding DME. The decrease in methanol selectivity and the increase in DME selectivity by the addition of STA to the catalyst structure was due to the increase in the Bronsted acidity with the addition of STA. Enhancement of CO conversion and DME selectivity could be explained by the surface acidity of the catalyst. From the DRIFTS analysis results of the catalysts, the highest Bronsted acidity was observed in the 25STA@CZA-MA catalyst. Based on the reaction stoichiometry (Equation (5)), the maximum possible DME and CO₂ selectivity values are about 66% and 33%, respectively. DME and the CO₂ selectivity values obtained with the 25STA@CZA-MA catalyst were 59.8% and 31.8%, respectively. These values were somewhat less than the values that would be predicted from the stoichiometry of the overall reaction (Equation (5)). This was

due to the presence of some methanol and a small amount of methane in the product stream. Methane production occurred due to the reverse dry reforming reaction. As the amount of STA in the structure of the core-shell-type catalyst was increased, a significant reduction was observed in the methanol mole fraction in the product stream (Figure 8). The incore-shell-type STA content from 5% to 25% also caused a significant increase in the fractional conversion of CO and hence DME yield.



(a)



(b)

Figure 7. (a) Comparison of activity test results with equilibrium conversion values predicted from thermodynamic analysis, (b) CO conversion values with the STA incorporated core-shell catalysts (feed stream = CO/H₂:1/1; P = 50 bar) (T = 275 °C; P = 50 bar; CO/H₂:1/1 as feed stream; space-time of 0.72 s.gcat/mL).

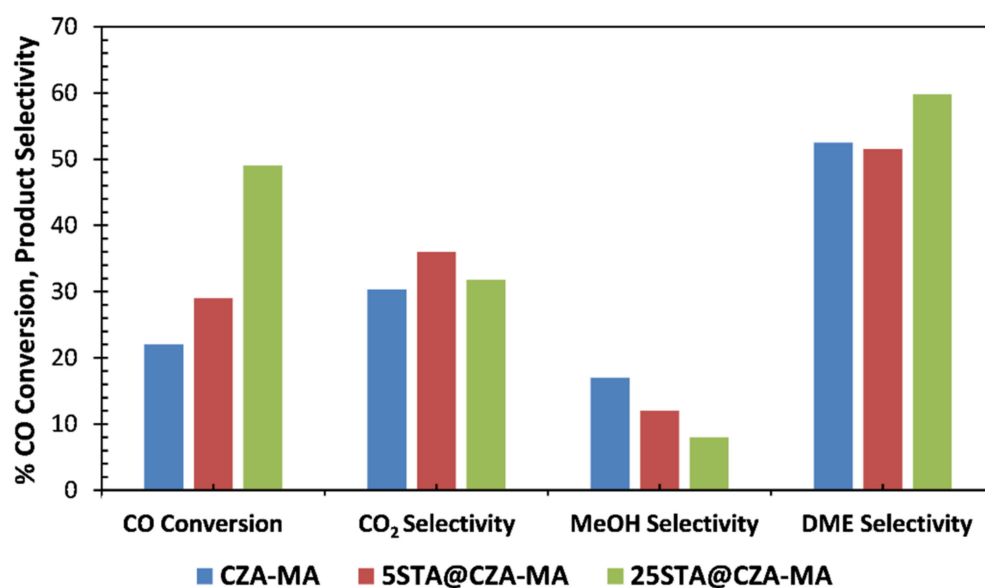


Figure 8. CO conversion and Product distribution of STA incorporated core-shell catalysts (T = 275 °C; P = 50 bar; CO/H₂:1/1 as feed stream; space-time of 0.72 s.gcat/mL).

Activity test results obtained in the present study with the STA impregnated core-shell-type catalysts were compared with the results reported in our earlier study, which was performed with a physically mixed methanol synthesis and STA-impregnated mesoporous alumina catalyst combination at 275 °C and 50 bar [14] (Table 3). Data from our previous studies were given in the Table 3. The same amount of STA was impregnated into mesoporous alumina in that work. Results showed the superiority of the core-shell-type catalytic material over the physically mixed catalyst combination for the fractional conversion of CO and the DME yield.

Table 3. The comparison of Activity Test Results of the STA incorporated bifunctional catalysts (T = 275 °C; P = 50 bar; CO/H₂:1/1 as feed stream).

Catalyst	CO Conversion, %	MeOH Selectivity, %	DME Selectivity, %	DME Yield, %
25STA@CZA-MA	49	8	59.8	29.3
STA@MA + MSC [14]	42	20	62	26.0
25STA@CZA [22]	28	8.7	59.1	16.5

Comparison of the results obtained in this work with the STA-impregnated core-shell-type catalytic material with the results reported in another earlier publication of our group with an STA incorporated CZA catalyst [22], also proved the superiority of the core-shell-type catalytic material (Table 3) in direct synthesis of DME. Results obtained here proved that STA was uniformly dispersed in the shell section of the core-shell-structured material and converted the formed methanol in the core section of the catalyst to DME more effectively.

2.3. Effects of Reaction Temperature and Pressure on Product Distribution

Direct synthesis of DME from syngas is a highly exothermic reaction (Equation (5)). Hence, equilibrium considerations favor lower temperatures. The best temperature range for the methanol synthesis reaction from syngas was reported as being in the range of 250–300 °C. Also, the stoichiometry of the DME synthesis reaction favors high pressures to achieve high conversions of CO. To determine the best reaction temperature and pressure for DME synthesis with the core-shell-type 25STA@CZA-MA catalyst, a set of experiments was performed in the temperature and pressure ranges of 200–300 °C and 30–50 bar, respectively.

As seen from the thermodynamic analysis results (Figure 7a), the conversion of CO decreases with an increase in temperature. However, in the catalytic activity test studies, CO conversion increased with an increase in temperature (Figure 9). This was simply due to the increase in the forward reaction rate with temperature. According to Arrhenius Law, the reaction rate increases as a function of temperature, resulting in significantly improved conversion. Figure 9 shows that with increasing temperature, both CO conversion and DME selectivity increased, while the carbon dioxide selectivity decreased from 40% to 32%. This was due to the exothermic nature of the water–gas shift reaction and the increase in the rate of the reverse of this reaction with an increase in temperature. The major products of the direct DME synthesis reaction (Equation (5)) are DME and CO₂. According to the stoichiometry of this overall reaction, one would expect similar trends for the temperature dependences of DME and CO₂ selectivities. However, the increase in temperature led to an increase in the rate of RWGS reaction, in which CO₂ is a reactant [41,42]. Moreover, temperatures higher than 300 °C are not suitable for DME production due to the thermodynamic limitations and stability of the bifunctional-catalyst. After 275 °C, CO conversion was leveled, mainly due to the catalyst deactivation caused by copper sintering at high temperatures [14].

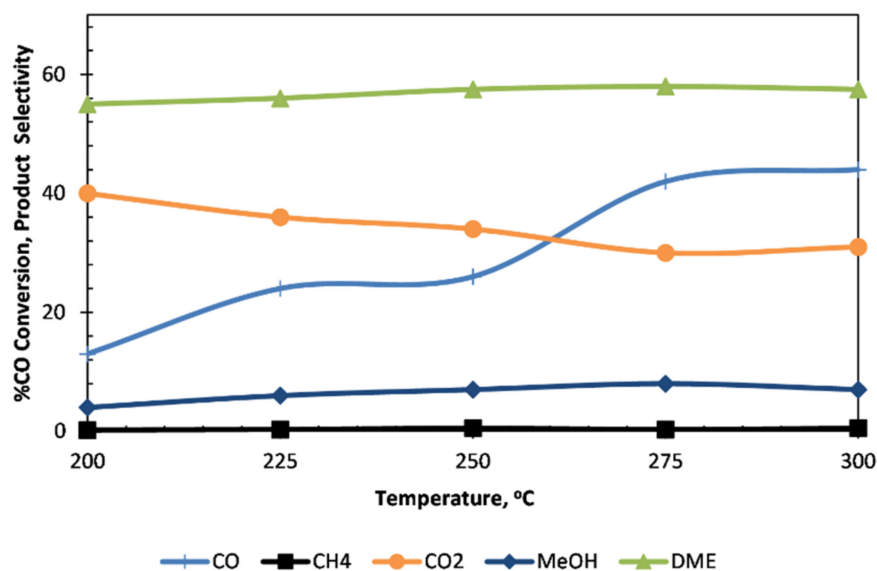


Figure 9. Effect of reaction temperature on CO conversion and product distribution (T = 200–300 °C; P = 50 bar; CO/H₂:1/1 as feed stream).

The effect of reaction pressure on CO conversion and product selectivity was also examined. As seen in Figure 10, the increase in pressure promoted CO conversion and DME selectivity. The CO conversion value was 12% at 30 bar. An increase in pressure to 50 bar improved the conversion to 49%. Considering the stoichiometry of the overall reaction (Equation (5)), the conversion of CO was expected to increase with an increase in the reaction pressure [43]. Hence, operating at high pressure is favored for the synthesis of DME from syngas. However, very high reaction pressure may have operational risks. Therefore, the reaction pressure was selected as 50 bar in the experiments performed for dry reforming of methane. Results obtained in this work with the 25STA@CZA-MA catalyst gave the highest DME selectivity and CO conversion values as 59.8% and 49%, respectively, at 50 bar and 275 °C.

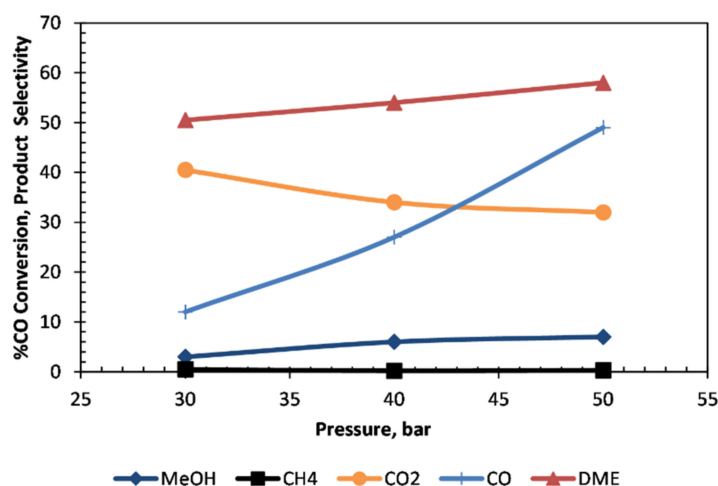


Figure 10. Effect of reaction pressure on product distribution ($T = 275\text{ }^{\circ}\text{C}$; $P = 30\text{--}50\text{ bar}$; $\text{CO}/\text{H}_2:1/1$ as feed stream).

2.4. Dimethyl Ether and Methanol Synthesis from Syngas in the Presence of CO_2

2.4.1. Methanol from CO_2

In our previous study, the methanol synthesis catalyst CZA was shown to give highly stable activity in the methanol synthesis reaction, with a feed stream containing a molar feed ratio of CO/H_2 as 1/1 [13]. The conversion of CO was determined as about 5% at $275\text{ }^{\circ}\text{C}$ and 50 bar pressure in that work.

In the case of experiments performed with CO_2 -containing gas mixtures, carbon dioxide also acts as a reactant, contributing to the formation of methanol. Hence, the conversion and the selectivity definitions given by Equations (14)–(19) should be used to determine the total conversion of $\text{CO}_2 + \text{CO}$ and the product selectivities based on the total conversion of $\text{CO} + \text{CO}_2$. Moreover, DME yield was calculated via Equation (20).

$$X_{\text{CO}} = \frac{F_{\text{CO}_{in}} - F_{\text{CO}_{out}}}{F_{\text{CO}_{in}}} \quad (14)$$

$$X_{\text{CO}_2} = \frac{F_{\text{CO}_2_{in}} - F_{\text{CO}_2_{out}}}{F_{\text{CO}_2_{in}}} \quad (15)$$

$$X_{\text{CO}+\text{CO}_2} = \frac{(F_{\text{CO}} + F_{\text{CO}_2})_{in} - (F_{\text{CO}} + F_{\text{CO}_2})_{out}}{(F_{\text{CO}} + F_{\text{CO}_2})_{in}} \quad (16)$$

$$S_{\text{DME}} = \frac{2(F_{\text{DME}})}{(F_{\text{CO}} + F_{\text{CO}_2})_{in} - (F_{\text{CO}} + F_{\text{CO}_2})_{out}} \quad (17)$$

$$S_{\text{MeOH}} = \frac{F_{\text{MeOH}}}{(F_{\text{CO}} + F_{\text{CO}_2})_{in} - (F_{\text{CO}} + F_{\text{CO}_2})_{out}} \quad (18)$$

$$S_{\text{CH}_4} = \frac{F_{\text{CH}_4}}{(F_{\text{CO}} + F_{\text{CO}_2})_{in} - (F_{\text{CO}} + F_{\text{CO}_2})_{out}} \quad (19)$$

$$Y_{\text{DME}} = X_{\text{CO}+\text{CO}_2} \times S_{\text{DME}} \quad (20)$$

Two sets of experiments were performed with the CO_2 -containing gas mixtures having different $\text{CO}/\text{CO}_2/\text{H}_2$ molar ratios, being 40/10/50, 25/25/50, 10/40/50, and with a gas mixture containing only CO_2 and hydrogen ($\text{CO}/\text{CO}_2/\text{H}_2 = -/50/50$). The first set of experiments was performed using the copper–zinc–alumina-based methanol synthesis catalyst (CZA), which was synthesized in the present study. In this set of experiments, the overall conversion of $\text{CO} + \text{CO}_2$ to methanol and product selectivities were analyzed. In the second set of experiments, the core-shell-type bifunctional 25STA@CZA-MA catalyst

was used. The overall conversion of CO + CO₂, as well as the product selectivities (DME, methanol, methane, etc.) were determined.

The activity test results obtained in the methanol synthesis reaction using the CZA catalyst are given in Table 4. CO conversion was only about 5% in the absence of CO₂ in the feed stream. The addition of CO₂ to the feed stream showed a positive effect on the total conversion of CO + CO₂. The total conversion of CO + CO₂ was increased from 11.2% to 32% as a result of the increase in the CO₂/CO ratio from 10/40 to 40/10. The formation of some methane was also observed in these experiments, together with the main product, methanol. Methane selectivity increased with an increase in the CO₂/CO ratio in the feed stream. The formation of methane was ascribed mainly to the occurrence of the methanation reaction (Equation (21)). Some contributions of reverse dry reforming reaction were also expected (Equation (8)).

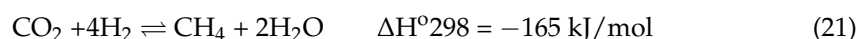


Table 4. Conversion values and product distribution of CZA catalysts for methanol synthesis at different feed compositions (T = 275 °C; P = 50 bar; space-time of 0.72 s.gcat/mL).

CO/CO ₂ /H ₂ Molar Ratio	Total Conversion, % (CO + CO ₂), %	MeOH Selectivity, %	CH ₄ Selectivity, %
40/10/50	11.2	97.7	2.3
25/25/50	21	85.3	14.7
10/40/50	32	83.6	16.4

Depending upon the composition of the feed stream, the water–gas shift reaction (WGSR) or reverse water–gas shift reaction (RWGSR) is expected to contribute to the product distribution. In the case of high values of CO₂/CO ratio, some carbon dioxide is expected to be converted to carbon monoxide by the RWGS reaction.

In the experiment performed with a feed stream containing only CO₂ as the carbon source (CO/CO₂/H₂ = -/50/50), the fractional conversion of carbon dioxide and the methanol selectivity values were found as 14.8% and 65.0%, respectively (Table 5). This conversion value was higher than the conversion obtained with a feed stream containing no CO₂ (CO/CO₂/H₂ = 50/-/50). The formation of CO and methane was observed together with the methanol synthesis reaction from CO₂. The CO and CH₄ selectivities were 24.7% and 10.3%, respectively, in this system. The formation of these side products was ascribed to the occurrence of reverse water–gas shift reaction and methanation reaction, respectively. These results supported the conclusion reported in the literature that methanol formation was mainly controlled by CO₂ hydrogenation [44].

Table 5. Experimental results obtained with the CZA catalyst with feed stream composition of CO/CO₂/H₂ = -/50/50 (T = 275 °C; P = 50 bar; space-time of 0.72 s.gcat/mL).

Catalyst	% CO ₂ Conversion, %	CH ₄ Selectivity, %	CO Selectivity, %	MeOH Selectivity, %
CZA	14.8	10.3	24.7	65.0

2.4.2. DME from CO₂

Experiments for the direct synthesis of DME from syngas were performed with the core-shell-type bifunctional 25STA@CZA-MA catalyst at 275 °C and 50 bar, with different CO/CO₂/H₂ molar ratios in the feed stream. The experiments that were performed in the absence of CO₂ (with a feed stream composition of CO/CO₂/H₂ = 50/-/50) gave CO conversion and DME selectivity values of 49% and 59.8%, respectively (Table 2). Some of the CO was converted to CO₂ in those tests, giving a CO₂ selectivity (based on converted CO) of 31.8%. In the case of feed streams containing both CO and CO₂, carbon dioxide may also act as a reactant for the production of DME and methanol. Hence, instead of individual

conversions of CO and CO₂, the total conversion of CO + CO₂ is defined and evaluated. Selectivities of the products were also defined with respect to the total converted amount of CO + CO₂ (Equations (14)–(19)).

Results reported in Table 6 show that the highest DME selectivity (88.7%) was obtained with a feed stream composition of CO/CO₂/H₂ = 40/10/50. The total conversion of CO + CO₂ and the DME yield values were 35.4% and 31.4%, respectively, for this feed stream composition. The increase in the CO₂/CO ratio of the feed stream caused some decrease in DME selectivity (Table 6). However, the total conversion of CO + CO₂ and DME yield increased with an increase in this ratio. The highest total conversion of CO + CO₂ and the DME yield values were obtained as 65.6% and 48%, respectively. Methane selectivity was close to zero in the case of CO hydrogenation reaction. However, higher methane selectivity values were observed with the addition of CO₂ into the feed stream. Apparently, CO₂ methanation reaction and the reverse dry reforming reaction of methane gain importance with an increase in the CO₂/CO ratio in the feed stream. These results are also illustrated in Figure 11. As shown in this figure, the maximum DME selectivity was obtained with the feed stream composition of CO/CO₂/H₂: 40/10/50. As the CO₂ content increased, DME selectivity decreased due to the synergic effect of DME reactions. As a result of the increase in CO₂/CO ratio in the feed stream, the reverse WGSR gains importance, and water formation takes place through this reaction. The increase in water concentration near the dehydration zone of the catalyst has a negative effect on the methanol dehydration reaction. Hence, some decrease in DME selectivity was observed. Moreover, a high water concentration causes hydrothermal degradation of methanol synthesis catalysts. For this reason, the deactivation of CZA catalysts could be determined during the activity test studies. As known from the literature survey, a high percentage of catalyst activity is lost in the first 1000 h of operation [34]. However, in this study, the core-shell model catalysts showed stable activity for 200 min. Moreover, the presence of the methanol synthesis catalyst in the core makes the copper more resistant to water. On the other hand, a significant increase was observed in the total conversion of CO + CO₂, as well as DME yield (which was evaluated by multiplying total conversion of CO + CO₂ with DME selectivity) with an increase in the CO₂/CO ratio.

Table 6. Conversion and product distribution of 25STA@CZA-MA catalysts for DME synthesis at different feed compositions (T = 275 °C; P = 50 bar; space-time of 0.72 s.gcat/mL).

CO/CO ₂ /H ₂ Molar Ratio	DME Selectivity, %	CH ₄ Selectivity, %	MeOH Selectivity, %	Total Conversion, % (CO + CO ₂)	DME Yield, %
40/10/50	88.7	2.5	8.8	35.4	31.4
25/25/50	79.6	6.4	14.0	48.0	38.2
10/40/50	73.2	10.8	16.0	65.6	48.0

As reported in the literature, different methanol synthesis and methanol dehydration catalysts were used for DME production from syngas. Also, physical mixtures of the methanol synthesis and the dehydration catalysts were used in many of the studies. HZSM-5 is one of the most preferred catalysts for methanol dehydration. It has high surface acidity and contains both strong Lewis and Bronsted acid sites. In the study of Ren, a physical mixture of zirconia-incorporated methanol synthesis catalyst (CZZA) and HZSM-5 catalyst was used for the CO₂ hydrogenation reaction [45]. The feed stream contained 25% CO₂ and 75% H₂ in that work. Quite high CO₂ conversion values, decreasing from 25% to 21%, were reported in a 100-h test. The corresponding DME selectivity values were in the range of 70–55%, at 240 °C and 28 bar [45]. In our study, the highest DME selectivity (88.7%) was obtained with a feed stream composition of CO/CO₂/H₂ = 40/10/50 using the new STA incorporated core-shell-type catalytic material. The total conversion of CO + CO₂ was 35.4%, for this feed stream composition.

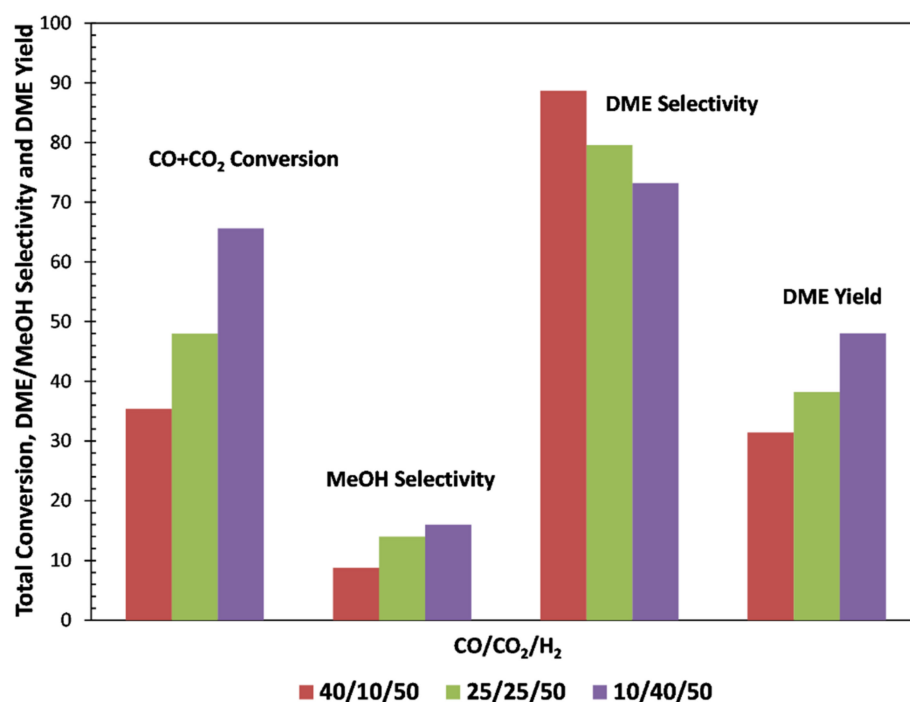


Figure 11. Total conversion, DME/MeOH selectivity, and DME yield of 25STA@CZA-MA catalysts at different feed composition (T = 275 °C; P = 50 bar; space-time of 0.72 s.gcat/mL).

Results reported in the study of Guo [46] with bifunctional CZA-HZSM-5 catalyst pairs (physical mixture, tablet, and coated) also indicated quite stable activity in 100-h tests at 250 °C and 30 bar, with a feed composition of CO/CO₂/H₂/N₂:36/18/36/10. CO conversion, CO₂ conversion, and DME selectivity values were reported as 54.5%, –39.0%, and 65.3%, respectively, with the coated catalyst.

Our experimental results were also compared with the studies conducted by Bayat et al., in which a physical mixture of commercial methanol synthesis catalyst and STA-loaded mesoporous alumina was used in DME production [14]. The DME selectivity (90%) and overall conversion of CO + CO₂ values, which were reported in that work with a feed stream composition of CO/CO₂/H₂: 40/10/50, were quite close to the values obtained in the present study. In another study, physical mixtures of commercial methanol synthesis catalyst with the STA incorporated silica-based TRC-75(L) dehydration catalyst were used in the direct synthesis of DME. Results reported at 275 °C and 50 bar with a feed composition of CO/CO₂/H₂: 40/10/50 gave a DME selectivity value of 70% and a CO conversion of about 20% [15]. These values were much less than the corresponding values obtained with the core-shell-type catalyst synthesized in the present study.

3. Materials and Methods

3.1. Catalyst Preparation

In this study, core-shell-type catalysts were developed for the direct synthesis of dimethyl ether from syngas and CO₂. While the core part of the synthesized catalyst is the methanol synthesis catalyst, the shell part consists of silicotungstic acid-incorporated mesoporous alumina, which is used for methanol dehydration. Mesoporous alumina is a suitable dehydration catalyst for DME synthesis reaction, as alumina possesses higher surface area, thermal stability, surface acidity, and uniform pore diameter distribution.

Core-shell-type catalysts were synthesized by a hydrothermal method. However, before the preparation of core-shell catalysts, the synthesis of a Cu/ZnO/Al₂O₃ (CZA) catalyst was performed. The CZA catalyst was prepared by a co-precipitation method. The molar ratio of the copper/zinc/alumina in the CZA catalyst was arranged as 6/3/1. Sodium carbonate was used as a co-precipitate agent. After the precipitation, the materials

were washed, dried, and calcined. The calcination process was performed under dry air at 350 °C for 6 h, at a heating rate of 1 K/min. Detailed information about the synthesis route and activity test results of the CZA catalysts in methanol synthesis were given in our previous study [22].

The hydrothermal method, which was used in the synthesis of the shell section of the core-shell-type catalyst, is similar to the method proposed by Ibrahim et al. [5]. All the chemicals were bought from Merck Millipore, Darmstadt, Germany. In this procedure, the alumina source (aluminum isopropoxide ($C_9H_{21}AlO_3$, Merck, 98%)) was dissolved in ethanol. Then, nitric acid (HNO_3 , Merck, 65%) was added to this solution to adjust the acidity. The resulting solution was stirred at room temperature for 6 h. In a separate vessel, Pluronic P123 ($EO_{20}PO_{70}EO_{20}$, Sigma-Aldrich) was dissolved in ethanol. Subsequently, this solution was added to the alumina solution and mixed at room temperature for 1 h to obtain a homogenous solution. The calcined CZA catalyst was then put into this homogenous solution. The weight ratio of the mesoporous alumina and CZA (CZA/MA) was adjusted as 1/1. The heterogeneous mixture was continuously stirred for 18 h. Then, it was placed in an oven at 60 °C for 2 days. The solid product was then calcined under dry air at 750 °C for 6 h. The catalyst that was synthesized using this method was named CZA-MA.

In order to increase the surface acidity of the core-shell-type catalysts, silicotungstic acid (STA) ($H_4(Si(W_3O_{10})_4) \cdot xH_2O$, Merck) was impregnated into the catalyst structure at 5% and 25% by mass. In this impregnation process, the CZA-MA catalyst was stirred in deionized water at room temperature. The desired amount of silicotungstic acid was dissolved in deionized water in a separate vessel. Then, the clear acid solution was added dropwise to the CZA-MA catalyst and stirred at 40 °C until all the water was vaporized. The solid sample was calcined using the same procedure as used with CZA-MA. As known from the literature, metallic copper (Cu^0) is the active site in the CZA catalyst for methanol synthesis [22]. For this reason, before the activity test studies, STA incorporated CZA-MA catalysts were reduced at 300 °C under hydrogen flow.

3.2. Catalyst Characterization

STA incorporated CZA-MA catalysts were characterized by X-ray diffraction, N_2 physisorption, Scanning Electron Microscopy with Energy Dispersive X-ray Spectroscopy (SEM-EDS), Inductively Coupled Plasma Mass Spectrometry (ICP-MS), pyridine-adsorbed diffuse reflectance FTIR spectroscopy (DRIFTS), Temperature Programmed Reduction (TPR), and HR-TEM techniques.

The surface area, pore diameter, and pore volume of the core-shell catalysts were determined by N_2 physisorption techniques using a Quanta Chrome Autosorb-1C sorptometer (Quantachrome Instruments, Boynton Beach, FL, USA). Before the analysis, synthesized catalysts were degassed at 120 °C for 6 h. XRD patterns of STA incorporated catalysts were performed using a Rigaku D/MAX 2200 device with a $Cu-K\alpha$ ($\lambda = 0.15406$ nm) source (Rigaku Corporation, Akishima-shi, Japan). The crystalline nature of the synthesized materials was analyzed in 2θ values ranging between 10° and 90° and with a speed of 2°/min. Scanning electron microscopy (SEM) analysis was performed with a Quanta 400F Field Emission SEM device to determine the surface morphologies (Quantachrome Instruments, Boynton Beach, FL, USA). SEM/EDX and ICP-MS analyses were carried out to determine active metal compositions. ICP-MS analyses were performed with the Perkin Elmer SCIEX ELAN DRC II instrument (Perkin-Elmer SCIEX, Concord, ON, Canada). Diffuse reflectance FT-IR spectra of the pyridine-adsorbed samples (DRIFTS) were recorded with a JASCO FT-IR/4700 spectrometer (JASCO, Deutschland) to determine the Lewis and Bronsted acid sites of the catalysts. The core-shell structures of the synthesized materials were determined by high-resolution transmission electron microscopy (HRTEM). TPR analysis was recorded using the ChemBET 3000 TPR/TPD instrument (Quantachrome Instruments, Boynton Beach, FL, USA) to determine the reduction temperature of active metals.

3.3. Direct Synthesis of Dimethyl Ether

The direct synthesis reaction of dimethyl ether was performed in a fixed-bed tubular reactor in the pressure and temperature ranges of 30–50 bar and 200–300 °C, respectively. Before the dimethyl ether synthesis reaction, the catalyst particles were reduced under H₂ flow. The reduced catalyst was in powder form, and the sizes of the core-shell-type particles were in the range of 7–10 µm. The mass of the catalyst placed into the stainless-steel reactor was 0.6 g. All streams on the reactor system were heated to 200 °C to avoid condensation of the products. The effect of feed stream composition on the product distribution and the total conversion of (CO + CO₂) were investigated. For this reason, DME synthesis was achieved with different CO/CO₂ molar ratios, as 50%CO-50%H₂, 10%CO₂-40%CO-50%H₂; 25%CO₂-25%CO-50%H₂, 40%CO₂-10%CO-50%H₂, and 50%CO₂-50%H₂. However, in the feed stream, the total flow rate (60 mL/min) and hydrogen flow rate values were kept constant. The total analysis time was 200 min.

The composition of the reactor effluent stream was determined using an Agilent 6890 N gas chromatograph, which was connected online to the reactor. This chromatograph was equipped with a TC detector and a Carbosphere column. The temperature program of the chromatographic oven was adjusted to a 5 min hold at 38 °C to detect CO, CO₂, and CH₄. After that hold period, the temperature was raised to 120 °C with a 3 K/min temperature ramp and remained at that temperature for 5 min. The total run time was approximately 37.3 min.

Before the reaction tests, calibration factors of the peaks corresponding to different species in a chromatogram were determined. During the activity test studies, the total molar flow rate of the outlet stream was evaluated from the total volumetric flow rate, which was measured at the exit of the gas chromatograph, in each run. The molar flow rates of CO and the carbon-containing species (CO₂, CH₄, MeOH, DME) were then determined using the calibration factors of the species. Also, a carbon balance was made around the reactor. Based on these data, conversion and selectivity values were calculated.

4. Conclusions

Results proved that STA incorporated core-shell-type bifunctional catalysts showed excellent performance in the conversion of syngas and CO₂ to dimethyl ether. Activity test results revealed that the addition of STA on core-shell catalysts highly enhanced the catalytic activity in terms of CO and CO₂ conversions. DME production by in situ dehydration of the synthesized methanol in the shell section of the core-shell-type catalyst facilitated the direct synthesis of DME from syngas. Results proved that the addition of CO₂ into the syngas had a positive effect on methanol and DME selectivity values. In the absence of CO₂, the highest CO conversion and DME selectivity values were obtained as 49% and 59.8%, respectively, at 275 °C and 50 bar with the core-shell-type 25STA@CZA-MA catalyst. However, the total conversion of CO + CO₂ and DME selectivity based on total conversion was 65% and 73.2%, respectively, over the same catalyst, with a feed stream composition of CO/CO₂/H₂ = 10/40/50. The highest methanol selectivity, which was observed with the Cu-ZnO-Al type CZA catalyst (core section of the bifunctional catalyst), and the highest DME selectivity with the core-shell-type 25STA@CZA-MA catalyst were 97.7% and 88.7%, respectively. HR-TEM analysis results indicated that the core-shell structure of the mesoporous alumina-encapsulated Cu-ZnO-Al (CZA) catalyst (CZA-MA) was successfully synthesized by the hydrothermal method. Results proved that the new STA incorporated core-shell-type bifunctional catalysts were highly promising for the conversion of CO₂-containing syngas to an alternative clean energy carrier, namely DME.

Author Contributions: Conceptualization, N.O., G.D. and T.D.; methodology, B.P.K. and N.O.; investigation, B.P.K.; writing—original draft preparation, B.P.K.; writing—review and editing, N.O., G.D. and T.D.; visualization, N.O. and G.D.; supervision, T.D.; project administration, N.O. All authors have read and agreed to the published version of the manuscript.

Funding: This research was financed by TUBITAK (115M377) and Gazi University Research Fund (06/2017-09 and 06/2018-23).

Data Availability Statement: The data presented in this study are available on request from the corresponding author.

Acknowledgments: The authors would like to thank the Central Laboratory of METU for the characterization results of the synthesized materials.

Conflicts of Interest: The authors declare no conflict of interest.

References

1. Olah, G.A.; Goepfert, A.; Prakash, G.K.S. *Beyond Oil and Gas: The Methanol Economy*; Wiley VCH Verlag GmbH & Co: Weinheim, Germany, 2006.
2. Stancin, H.; Mikulcic, H.; Wang, X.; Duric, N. A review on alternative fuels in future energy system. *Renew. Sustain. Energy Rev.* **2020**, *128*, 109927. [[CrossRef](#)]
3. Dogu, T.; Varisli, D. Alcohols as alternatives to petroleum for environmentally clean fuels and petrochemicals. *Turk. J. Chem.* **2007**, *31*, 551–555.
4. Azizi, Z.; Rezaeimanesh, M.; Tohidian, T.; Rahimpour, M.R. Dimethyl Ether: A review of technologies and production challenges. *Chem. Eng. Process.* **2014**, *82*, 150. [[CrossRef](#)]
5. Ibrahim, S.A.; Ekinci, E.K.; Karaman, B.P.; Oktar, N. Coke-resistance enhancement of mesoporous γ -Al₂O₃ and MgO-supported Ni-based catalysts for sustainable hydrogen generation via steam reforming of acetic acid. *Int. J. Hydrogen Energy.* **2021**, *46*, 38281–38298. [[CrossRef](#)]
6. Smyrniot, M.; Ioannides, T. Dimethyl Ether Hydrolysis over WO₃/ γ -Al₂O₃ Supported Catalysts. *Catalysts* **2022**, *12*, 396. [[CrossRef](#)]
7. Semelsberger, T.A.; Borup, R.L.; Greene, H.L. Dimethyl ether (DME) as an alternative fuel. *J. Power Sources* **2006**, *156*, 497–511. [[CrossRef](#)]
8. Erena, J.; Garona, R.; Arandes, J.M.; Aguayo, A.T.; Bilbao, J. Effect of operating conditions on the synthesis of dimethyl ether over a CuO-ZnO-Al₂O₃/NaHZSM-5 bifunctional catalyst. *Catal. Today* **2005**, *107–108*, 467–473. [[CrossRef](#)]
9. Bae, J.W.; Kang, S.H.; Lee, Y.J.; Jun, K.W.J. Effect of precipitants during the preparation of Cu-ZnO-Al₂O₃/Zr-ferrierite catalyst on the DME synthesis from syngas. *J. Ind. Eng. Chem.* **2009**, *15*, 566–572. [[CrossRef](#)]
10. Woo, J.; Jun, Y.; Ho, S.; Yoo, P.J.; Lee, D.H.; Jun, K.W.; Bae, W.B. Effect of copper surface area and acidic sites to intrinsic catalytic activity for dimethyl ether synthesis from biomass-derived syngas. *Appl. Catal. B Environ.* **2012**, *126*, 1–8.
11. Song, F.; Tan, Y.; Xie, H.; Zhang, Q.; Han, Y. Direct synthesis of dimethyl ether from biomass-derived syngas over Cu-ZnO-Al₂O₃-ZrO_{2(x)}/ γ -Al₂O₃ bifunctional catalysts: Effect of Zr-loading. *Fuel Process. Technol.* **2014**, *126*, 88–94. [[CrossRef](#)]
12. Zhang, M.; Liu, Z.; Lin, G.; Zhang, H. Pd/CNT-promoted Cusingle bond ZrO₂/HZSM-5 hybrid catalysts for direct synthesis of DME from CO₂/H₂. *Appl. Catal. A Gen.* **2013**, *451*, 28–35. [[CrossRef](#)]
13. Gao, W.; Wang, H.; Wang, Y.; Guo, W.; Jia, M. Dimethyl ether synthesis from CO₂ hydrogenation on La-modified CuO-ZnO-Al₂O₃/HZSM-5 bifunctional catalysts. *J. Rare Earths* **2013**, *31*, 470–476. [[CrossRef](#)]
14. Bayat, A.; Dogu, T. Optimization of CO₂/CO Ratio and Temperature for Dimethyl Ether Synthesis from Syngas over a New Bifunctional Catalyst Pair Containing Heteropolyacid Impregnated Mesoporous Alumina. *Ind. Eng. Chem. Res.* **2016**, *55*, 11431–11439. [[CrossRef](#)]
15. Celik, G.; Arinan, A.; Bayat, A.; Ozbelge, H.O.; Dogu, T.; Varisli, D. Performance of Silicotungstic Acid Incorporated Mesoporous Catalyst in Direct Synthesis of Dimethyl Ether from Syngas in the Presence and Absence of CO₂. *Topics Catal.* **2013**, *56*, 1764–1774. [[CrossRef](#)]
16. Ateka, A.; Perez-Uriarte, P.; Gamero, M.; Erena, J.; Aguayo, A.T.; Bilbao, J. A comparative thermodynamic study on the CO₂ conversion in the synthesis of methanol and of DME. *Energy* **2017**, *120*, 796–804. [[CrossRef](#)]
17. Jia, G.; Tan, Y.; Han, Y. A comparative study on the thermodynamics of dimethyl ether synthesis from CO hydrogenation and CO₂ hydrogenation. *Ind. Eng. Chem. Res.* **2006**, *45*, 1152–1159. [[CrossRef](#)]
18. Mota, N.; Ordonez, E.M.; Paweled, B.; Fierro, J.L.G.; Navarro, R.M. Direct Synthesis of Dimethyl Ether from CO₂: Recent Advances in Bifunctional/Hybrid Catalytic Systems. *Catalysts* **2021**, *11*, 411. [[CrossRef](#)]
19. Contador, M.S.; Ateka, A.; Ibane, M.; Bilbao, J.; Aguayo, A.T. Influence of the operating conditions on the behavior and deactivation of a CuO-ZnO-ZrO₂@SAPO-11 core-shell-like catalyst in the direct synthesis of DME. *Renew. Energy* **2019**, *138*, 585–597. [[CrossRef](#)]
20. Han, F.; Liu, H.; Cheng, W.; Xu, Q. Highly selective conversion of CO₂ to methanol on the CuZnO-ZrO₂ solid solution with the assistance of plasma. *RSC Adv.* **2020**, *10*, 33620. [[CrossRef](#)]
21. Lei, H.; Nie, R.; Wu, G.; Hou, Z. Hydrogenation of CO₂ to CH₃OH over Cu/ZnO catalysts with different ZnO morphology. *Fuel* **2015**, *154*, 161–166. [[CrossRef](#)]
22. Karaman, B.P.; Oktar, N.; Dogu, G.; Dogu, T. Bifunctional silicotungstic acid and tungstophosphoric acid impregnated Cu-Zn-Al & Cu-Zn-Zr catalysts for dimethyl ether synthesis from syngas. *Catal. Lett.* **2020**, *150*, 2744–2761.

23. Wang, G.; Mao, D.; Guo, X. Enhanced performance of the CuO–ZnO–ZrO₂ catalyst for CO₂ hydrogenation to methanol by WO₃ modification. *Appl. Surf. Sci.* **2018**, *456*, 403–409. [[CrossRef](#)]
24. Xiao, J.; Mao, D.; Guo, X.; Yu, J. Effect of TiO₂, ZrO₂, and TiO₂–ZrO₂ on the performance of CuO–ZnO catalyst for CO₂ hydrogenation to methanol. *Appl. Surf. Sci.* **2015**, *338*, 146–153. [[CrossRef](#)]
25. Fornero, E.L.; Sanguineti, P.B.; Chiavassa, D.L.; Bonivardi, A.L.; Baltanas, M.A. Performance of ternary Cu–Ga₂O₃–ZrO₂ catalysts in the synthesis of methanol using CO₂-rich gas mixtures. *Catal. Today* **2013**, *213*, 163–170. [[CrossRef](#)]
26. Wang, W.; Qu, Z.; Song, L.; Fu, Q. CO₂ hydrogenation to methanol over Cu/CeO₂ and Cu/ZrO₂ catalysts: Tuning methanol selectivity via metal-support interaction. *J. Energy Chem.* **2020**, *40*, 22–30. [[CrossRef](#)]
27. Ciftci, A.; Varisli, D.; Tokay, C.K.; Sezgi, A.N.; Dogu, T. Dimethyl ether, diethyl ether & ethylene from alcohols over tungstophosphoric acid based mesoporous catalysts. *Chem. Eng. J.* **2012**, *207–208*, 85–93.
28. Ozcan, M.C.; Karaman, B.P.; Oktar, N.; Dogu, T. Dimethyl ether from syngas and effect of CO₂ sorption on product distribution over a new bifunctional catalyst pair containing STA@SBA-15. *Fuel* **2022**, *330*, 125607. [[CrossRef](#)]
29. Ciftci, A.; Varisli, D.; Dogu, T. Dimethyl Ether Synthesis over Novel Silicotungstic Acid Incorporated Nanostructured Catalysts. *Int. J. Chem. React. Eng.* **2010**, *8*. [[CrossRef](#)]
30. Yang, G.; Tsubaki, N.; Shamoto, J.; Yoneyama, Y.; Zhang, Y. Confinement effect and synergistic function of H-ZSM-5/Cu–ZnO–Al₂O₃ capsule catalyst for one-step controlled synthesis. *J. Am. Chem. Soc.* **2010**, *132*, 8129–8136. [[CrossRef](#)]
31. Liu, R.; Tian, Y.; Yang, A.; Zha, F.; Ding, J.; Chang, Y. Preparation of HZSM-5 membrane packed CuO–ZnO–Al₂O₃ nanoparticles for catalysing carbon dioxide hydrogenation to dimethyl ether. *Appl. Surf. Sci.* **2015**, *345*, 1–9. [[CrossRef](#)]
32. Wang, Y.; Wang, W.; Chen, Y.; Ma, J.; Li, R. Synthesis of dimethyl ether from syngas over core–shell structure catalyst CuO–ZnO–Al₂O₃@SiO₂–Al₂O₃. *Chem. Eng. J.* **2014**, *250*, 248–256. [[CrossRef](#)]
33. Karaman, B.P.; Oktar, N. Tungstophosphoric acid incorporated hierarchical HZSM-5 catalysts for direct synthesis of dimethyl ether. *Int. J. Hydrogen Energy* **2020**, *45*, 34793–34804. [[CrossRef](#)]
34. Bartholomew, C.H.; Farrauto, R.J. *Fundamentals of Industrial Catalytic Processes*, 2nd ed.; Wiley: Hoboken, NJ, USA, 2006; p. 966.
35. Koh, M.K.; Wong, Y.J.; Chai, S.P.; Mohamed, A.R. Carbon dioxide hydrogenation to methanol over multi-functional catalyst: Effects of reactants adsorption and metal-oxide(s) interfacial area. *J. Ind. Eng. Chem.* **2017**, *62*, 156–165. [[CrossRef](#)]
36. Arbag, H. Effect of Impregnation Sequence during Synthesis Procedure on Performances of Bimetallic Ni-Co Catalysts in Dry Reforming of Methane. *J. Uludağ Uni. Eng. Fac.* **2017**, *22*, 39–52.
37. Akansu, H.; Arbag, H.; Tasdemir, H.M.; Yasyerli, S.; Yasyerli, N.; Dogu, G. Nickel-based alumina supported catalysts for dry reforming of biogas in the absence and the presence of H₂S: Effect of manganese incorporation. *Catal. Today* **2022**, *397–399*, 37–49.
38. Tangcharoen, T.; Klysubun, W.; Kongmark, C. Synchrotron X-ray absorption spectroscopy and cation distribution studies of NiAl₂O₄, CuAl₂O₄ and ZnAl₂O₄ nanoparticles synthesized by sol-gel auto combustion method. *J. Mol. Struct.* **2019**, *1182*, 219–229. [[CrossRef](#)]
39. Lee, S.; Lee, S.K.; Kim, S.; Yoon, K.; Han, S.; Lee, M.H.; Ko, Y.; Noh, J.H. Design of a lithiophilic and electron-blocking interlayer for dendrite-free lithium-metal solid-state batteries. *Science* **2022**, *8*, 30. [[CrossRef](#)]
40. Erena, J.; Garona, R.; Arandes, M.; Aguayo, A.; Bilbao, J. Direct Synthesis of Dimethyl Ether From (H₂+CO) and (H₂+CO₂) Feeds. Effect of Feed Composition. *Int. J. Chem. React. Eng.* **2005**, *3*. [[CrossRef](#)]
41. Phienluphon, R.; Pinkaew, K.; Yang, G.; Li, J.; Wei, Q. Designing core (Cu/ZnO/Al₂O₃)–shell (SAPO-11) zeolite capsule catalyst with a facile physical way for dimethyl ether direct synthesis from syngas. *Chem. Eng. J.* **2015**, *270*, 605–611. [[CrossRef](#)]
42. Otalvaro, N.D.; Otalvaro, G.; Delgado, K.H.; Wild, S.; Pitter, S.; Sauer, J. Kinetics of the direct DME synthesis from CO₂ rich syngas under variation of the CZA–Al₂O₃ ratio of a mixed catalyst bed. *RSC Adv.* **2021**, *11*, 24556. [[CrossRef](#)]
43. Moradi, G.; Ahmadpour, J.; Yari pour, F.; Wang, J. Equilibrium calculations for direct synthesis of dimethyl ether from syngas. *Can. J. Chem. Eng.* **2011**, *1*, 108–115. [[CrossRef](#)]
44. Dou, M.; Zhang, M.; Chen, Y. Theoretical study of methanol synthesis from CO₂ and CO hydrogenation on the surface of ZrO₂ supported In₂O₃ catalyst. *Surf. Sci.* **2018**, *672–673*, 7–12. [[CrossRef](#)]
45. Ren, S.; Fan, X.; Shang, Z.; Shoemaker, W.R.; Ma, L.; Wu, T.; Liang, X. Enhanced catalytic performance of Zr modified CuO/ZnO/Al₂O₃ catalyst for methanol and DME synthesis via CO₂ hydrogenation. *J. CO₂ Util.* **2020**, *36*, 82–95. [[CrossRef](#)]
46. Guo, X.; Liu, F.; Hua, Y.; Xue, H.; Yu, J.; Mao, D.; Rembel, G.Y.; Ng, F.T. One-step synthesis of dimethyl ether from biomass-derived syngas on CuO–ZnO–Al₂O₃/HZSM-5 hybrid catalyst: Combination method, synergistic effect, water-gas shift reaction and catalytic performance. *Catal. Today* **2022**, in press. [[CrossRef](#)]